Localized transversal-rotational modes in linear chains of equal masses

H. Pichard,[*] A. Duclos, J.-P. Groby, V. Tournat, and V. E. Gusev[†]

LAUM, UMR No. 6613 associée au CNRS, Université du Maine, Avenue O. Messiaen, 72085 Le Mans, France

The propagation and localization of transversal-rotational waves in a two-dimensional granular chain of equal masses are analyzed in this study. The masses are infinitely long cylinders possessing one translational and one rotational degree of freedom. Two dispersive propagating modes are predicted in this granular crystal. By considering the semi-infinite chain with a boundary condition applied at its beginning, the analytical study demonstrates the existence of localized modes, each mode composed of two evanescent modes. Their existence, position (either in the gap between the propagating modes or in the gap above the upper propagating mode), and structure of spatial localization are analyzed as a function of the relative strength of the shear and bending interparticle interactions and for different boundary conditions. This demonstrates the existence of a localized mode in a semi-infinite monatomic chain when transversal-rotational waves are considered, while it is well known that these types of modes do not exist when longitudinal waves are considered.

PACS number(s): 78.67.Pt, 45.70.−n, 63.20.Pw

I. INTRODUCTION

Many investigations have been devoted to the propagation of acoustic and elastic waves in periodic samples such as superlattices, multilayered structures, and phononic crystals in particular because of the presence of frequency band gaps, in which only nonpropagating waves can be excited. These waves, called evanescent waves, are particular solutions of the wave equation that decay or increase exponentially with distance. They are involved in many physical phenomena including coupling in and out of waveguides and resonators [1], near-field optics [2], tunneling [3,4], subwavelength focusing [5], or surface waves [6,7]. The question of the existence or nonexistence of localized vibrations and surface acoustic waves is of large interest in mechanics and acoustics because of the important role played by these modes in various physical processes [8–10]. It was shown that localized modes may be excited and associated with local defects of periodicity or with the ends of the lattice. The case of a localized mode occurring in one-dimensional (1D) monatomic [11,12] and diatomic [12–14] lattices has been studied previously for compressional waves. The localized modes engendered by an impurity of mass and force constant different from those of the atom it replaces in the chain have been characterized. As a results of these works, it is well known that in a semi-infinite linear chain of atoms, the vibrations cannot be localized near the free edge if all the masses and interactions between the neighboring atoms are equal. However, in this 1D lattice with a single degree of freedom, the localized vibrations exist near the first mass of the chain when the masses take alternatively two different values and the chain starts from a lighter mass. By modifying also the force constant of the impurity, the frequency of the localized mode can lie either in the forbidden frequency band between optical and acoustic branches or above the optical branch [13].

The localized vibration modes in periodically layered infinite and semi-infinite superlattices (SLs) have also

attracted increasing attention over the years. In particular, an inhomogeneity embedded in a SL with perfect periodicity (e.g., a defect, a free surface, or an interaction with a substrate) is shown to cause localized vibrations within the frequency gaps induced by the periodicity of a SL. Evidence of these modes has been demonstrated both theoretically [15,16] and experimentally via Raman spectroscopy [17], a phonon reflection experiment [18], and picosecond ultrasonic measurements [19,20].

More recently, the understanding and control of these localized modes have been reported in a 1D diatomic granular chain excited longitudinally. The granular chain consists of closely packed ensembles of elastically interacting particles. In these diatomic chains, where the beads are coupled by a spring responding to compression and dilatation, a band gap exists between the optical and acoustic propagating branches. Under certain conditions, depending on the parity of the number and on the characteristics (mass and diameter) of the beads in the chain, it was shown both theoretically [21–23] and experimentally [22–24] that one or two localized modes exist in these forbidden bands. Intrinsic localized modes, which are also known as discrete breathers, have also been reported in compressed 1D nonlinear diatomic granular crystals [25–27].

Here we demonstrate theoretically that a localized mode exists in a 2D monatomic granular phononic crystal composed of infinitely long cylinders with equal masses. The considered mechanical system possesses one translational and one rotational degree of freedom and the contacts between the cylinders are provided by linear shear and linear bending rigidities. In these granular crystals the elastic contacts between adjacent particles occur over a surface that is much smaller than the particle dimensions and much softer than the particles themselves. This enables the propagation of elastic waves at frequencies much lower than the acoustic resonance frequencies of the individual particles [28,29]. The problem considered could be realized experimentally, for instance, using a chain composed of short magnetic cylinders. To investigate the vibrational response of the chain, it can be excited at one of its ends by a shaker. The attractive magnetic force between cylinders causes in this case the prestress of the contacts between the

---

*helene.pichard.etu@univ-lemans.fr
†vitali.goussev@univ-lemans.fr

cylinders, initiating their shear and bending contact rigidities [30]. Two dispersive propagating acoustic modes, in which the rotational and transversal motions are mixed, are predicted in this granular phononic crystal. These modes are separated by a gap of forbidden frequencies. By considering a semi-infinite chain with different boundary conditions, we establish the necessary criteria for the existence of a localized mode. Simple analytical expressions are obtained for the propagating and localized modes, which provide the opportunity for a straightforward evaluation of the existence and the frequency of the localized mode. With the use of free boundary condition and when the structure is not composed of empty cylindrical shells, the frequency of the localized vibration, composed of the two evanescent acoustic modes, is located inside the low-frequency gap for waves propagation. Localization is also demonstrated with the use of more rigid boundary conditions. In this case the frequencies of the localized modes lie either in the forbidden band between the two propagating modes or above the upper propagating mode. It is worth mentioning that each of the localized coupled transversal and rotational modes in the evaluated chain of cylinders is composed of two evanescent modes. This is an important difference from earlier studied cases of longitudinal localized modes in linear chains of beads [21–23] and in layered structures [11,12], where at each frequency only a single evanescent mode could exist.

The results of our research are complementary to the recent theoretical [28,31,32] and experimental [33] investigations of the acoustic waves in 2D and 3D granular crystals possessing rotational degrees of freedom. The Cosserat theory predicts the existence of additional rotational bulk elastic modes [34,35] and the existence of additional surface acoustic waves with purely horizontal polarization of shear displacements [36], which are absent in the classical theory of elasticity of isotropic solids. Recently, the experimental observation of the coupled rotational-translational bulk modes in a noncohesive granular phononic crystal [33] was reported. It was also demonstrated that the Cosserat theory in general fails to predict correctly the dispersion relations of the bulk elastic modes in granular crystals even in the long-wavelength limit because it does not account for all effects of the material in-homogeneity on its elastic behavior. A remarkable interaction between longitudinal, transversal, and rotational motions of the particles was demonstrated theoretically [32], leading to a complete band gap, the Dirac cone and to the existence of zero-energy rotational vibrations. These investigations were conducted in search of potential application of these crystals as phononic metamaterials for shear wave control. The investigations described below were also inspired by the currently growing general interest in edge and surface waves of various physical natures [37–41], which is stimulated by the progress in the understanding of topological insulators.

The theoretical analysis of the propagation in an infinite chain of a cylinder is presented in Sec. II. Then the study focuses on the search for the possible localized modes in the chain. Their existence, general position (within the gap between the propagating modes or the gap above the upper propagating mode), and localization structure are analyzed in Sec. III for different boundary conditions applied at the beginning of the chain.
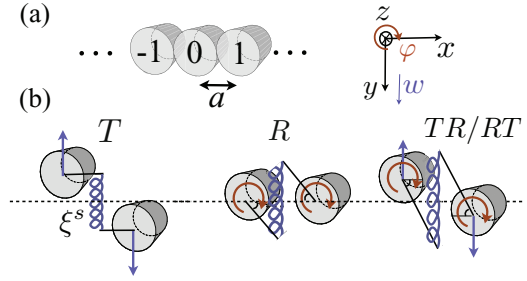

FIG. 1. (Color online) (a) Representation of the infinite linear granular chain. (b) Illustration of different possible motions.

II. INFINITE LINEAR GRANULAR CHAIN

A. Theory

The 2D linear chain under consideration is made of infinitely long cylinders with a circular cross section, as depicted in Fig. 1(a). The structure is characterized by a lattice constant $a = 2R_c$, where R_c is the radius of the cylinders. Each cylinder possesses one translational and one rotational degree of freedom. The shear force at the contact between two adjacent particles is described by a spring of constant rigidity ξ^s. The elongation of the springs introduces forces and momenta that induce the motion of the particles: the displacement w along the y axis and the rotation φ around the z axis [Fig. 1(b)]. Here T and R indicate purely transversal and rotational motions, respectively, and TR and RT refer to coupled transversal-rotational modes with a predominance of translation or a predominance of rotation, respectively.

The equations of motion of the zeroth particle obtained by applying the Lagrange principle [42] are

$$m\ddot{w}_0 = -\xi^s(\delta s_{-1} - \delta s_1), \tag{1a}$$

$$I\ddot{\varphi}_0 = -\xi^s R_c(\delta s_{-1} + \delta s_1), \tag{1b}$$

where m is the mass of the cylinder and I is its inertia momentum. The shear spring elongations, i.e., the relative displacements between the zeroth particle and its neighboring particles at the contact points, are denoted by δs_n, with n the particle number, and are explicitly given by

$$\delta s_{-1} = w_0 - w_{-1} + R_c(\varphi_0 + \varphi_{-1}), \tag{2a}$$

$$\delta s_1 = w_1 - w_0 + R_c(\varphi_1 + \varphi_0). \tag{2b}$$

The bending rigidity at the contacts of radius r is described by two additional springs with normal rigidities ξ^B (Fig. 2). They are located at the edge points of the contacts and are oriented orthogonally to the contact surface. The resulting additional momenta acting on the zeroth particle are described
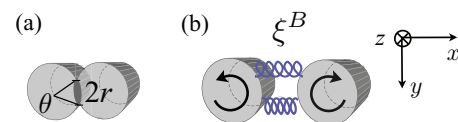

FIG. 2. (Color online) Schematic representation of the bending rigidity: (a) contact geometry and (b) bending coupling.

by $M_{0n} = -\frac{(R_c\theta)^2}{2}\xi^B(\varphi_0 - \varphi_n)$, with $n = -1, 1$ and θ the angular contact dimension. The radius of the contact is defined by $r = \frac{R_c\theta}{2}$.

The equation of motion for the rotation (1b) is then modified to account for all additional momenta $\Delta M = -\frac{(R_c\theta)^2}{2}\xi^B(2\varphi_0 - \varphi_{-1} - \varphi_1)$ applied on the zeroth particle.

The equations of motion become

$$m\ddot{w}_0 = -\xi^s[2w_0 - w_{-1} - w_1 + R_c(\varphi_{-1} - \varphi_1)], \quad (3)$$

$$I\ddot{\varphi}_0 = -\xi^s R_c[w_1 - w_{-1} + R_c(2\varphi_0 + \varphi_{-1} + \varphi_1)]$$
$$- \frac{(R_c\theta)^2}{2}\xi^B(2\varphi_0 - \varphi_{-1} - \varphi_1). \quad (4)$$

Their solutions are sought in the form of plane waves

$$\mathbf{V}_n = \begin{pmatrix} w_n(x,t) \\ \Phi_n(x,t) \end{pmatrix} = \mathbf{v}e^{i\omega t - ik_x x_n}, \quad (5)$$

with the new variable $\Phi = R_c\varphi$, k_x the complex wave number in the x direction, and $\mathbf{v} = \begin{pmatrix} A_w \\ A_\Phi \end{pmatrix}$ the amplitude vector. Equation (5) is developed around the equilibrium position x_0 of the central particle $\mathbf{V}_n = \mathbf{v}e^{i\omega t - ik_x x_0}e^{-ik_x \Delta x_n}$, where

$\Delta x_n = x_n - x_0$ is the relative coordinate between the central particle and the nth particle and ω is the angular frequency.

Finally, the substitution of Eq. (5) into the set of equations (3) and (4) leads to the eigenvalue problem

$$\mathbf{S}\mathbf{v} = -\Omega^2\mathbf{v}, \quad (6)$$

where $\Omega = \omega/\omega_0$ is the reduced frequency with $\omega_0 = 2\sqrt{\xi^s/m}$ and $\mathbf{S}$ is the dynamical matrix defined by

$$\mathbf{S} = \begin{pmatrix} -\sin^2 q & -i\sin q\cos q \\ ip\sin q\cos q & -p(\cos^2 q + p_B\sin^2 q) \end{pmatrix},$$

where $p_B = \frac{\theta^2}{2}\frac{\xi^B}{\xi^s}$ is the bending rigidity parameter, $p = \omega_1^2/\omega_0^2 = mR_c^2/I$ with $\omega_1 = 2R_c\sqrt{\xi^s/I}$, and $q = k_x a/2$ is the normalized wave number. Physically, the value of the parameter p is equal to or larger than 1. Depending on the mass distribution, the cylinders can be radially inhomogeneous ($I \leqslant mR^2$) and the limit case of $p = 1$ corresponds to a chain made of cylindrical infinitely thin shells.

The eigenvalue problem (6) can be solved for either Ω or $\sin q$. When Ω is the unknown, the solution of this eigenvalue problem gives the dispersion curves $\Omega = \Omega(q)$. There exist two possible values of $\Omega_\pm^2$ for a given wave number q, i.e., two modes defined by the square roots of the mathematical expression

$$\Omega_\pm^2 = \frac{1}{2}\{\sin^2 q + p(\cos^2 q + p_B\sin^2 q) \pm \sqrt{[\sin^2 q + p(\cos^2 q + p_B\sin^2 q)]^2 - 4p_B p\sin^4 q}\}. \quad (7)$$

Alternatively, when $\sin^2 q$ is the unknown, there exist two values of $S_\pm^2 = \sin^2 q_\pm$ and thus two wave numbers $q_\pm$ for a given frequency Ω,

$$S_\pm^2 = \sin^2 q_\pm = \Omega^2\frac{1 + p(p_B - 1)}{2p_B p}\left(1 \pm \sqrt{1 - \frac{4p_B p(\Omega^2 - p)}{\Omega^2[1 + p(p_B - 1)]^2}}\right) \quad \text{with} \quad p_B \neq 0. \quad (8)$$

The displacement and rotation of the two modes can then be written in the form

$$\begin{pmatrix} w_{n_\pm} \\ \Phi_{n_\pm} \end{pmatrix} = \begin{pmatrix} A_{w_\pm} \\ A_{\Phi_\pm} \end{pmatrix} e^{-i2q_\pm n}e^{i\omega t}$$
$$= A_{\Phi_\pm}\begin{pmatrix} \alpha_\pm \\ 1 \end{pmatrix} e^{-i2q_\pm n}e^{i\omega t}, \quad (9)$$

with $\alpha_\pm$ the ratio between the transversal $A_{w_\pm}$ and rotational $A_{\Phi_\pm}$ amplitudes of the modes defined by

$$\alpha_\pm = \frac{A_{w_\pm}}{A_{\Phi_\pm}} = \frac{iS_\pm C_\pm}{\Omega^2 - S_\pm^2}, \quad (10)$$

where $C_\pm^2 = \cos^2 q_\pm$, and n the particle number.

Equation (7) describes the $\Omega = \Omega(q)$ dispersion of the propagative and evanescent waves in the structure. When the solutions for the wave number q, determined by Eq. (8), are purely real, the waves are propagative. Evanescent waves whose frequency lies in the forbidden band for propagating waves are characterized by a complex-valued wave number in such a way that the amplitude of the mode should decay when it penetrates the chain. In this case, Eq. (7) describes the dispersion of waves that are attenuated to the right when n increases and to the left when n decreases.

Equation (7) is periodic and can be limited to a normalized wave number q value lying between 0 and $\frac{\pi}{2}$. In this study, the analysis is restricted to the first Brillouin zone and waves propagating to the right ($q > 0$).

B. Dispersion curves of the propagating modes

Figure 3 describes the $\Omega = \Omega(q)$ dispersion curves of the propagating modes depending on the value of the bending rigidity parameter p_B. The dispersion curves are restricted to a real wave number, i.e., to a wave propagating to the right (the positive direction). The eigenmodes of the granular chain motion are composed of two components, the transversal motion T and the rotational motion R. In Fig. 3, the plotted eigenvalues are colored relative to the type of associated eigenvectors that have been classified and the nature of the modes is labeled. Coupled transversal-rotational modes propagate in the chain: the solid red lines correspond to the modes with a predominance of rotation (RT) and the dashed blue lines correspond to the modes with a predominance of translation (TR). The frequencies of the modes at the edge of the Brillouin zone, i.e., at normalized wave numbers $q = 0$ and $q = \pi/2$, are found analytically and are indicated to emphasize the dependence of these characteristic frequencies
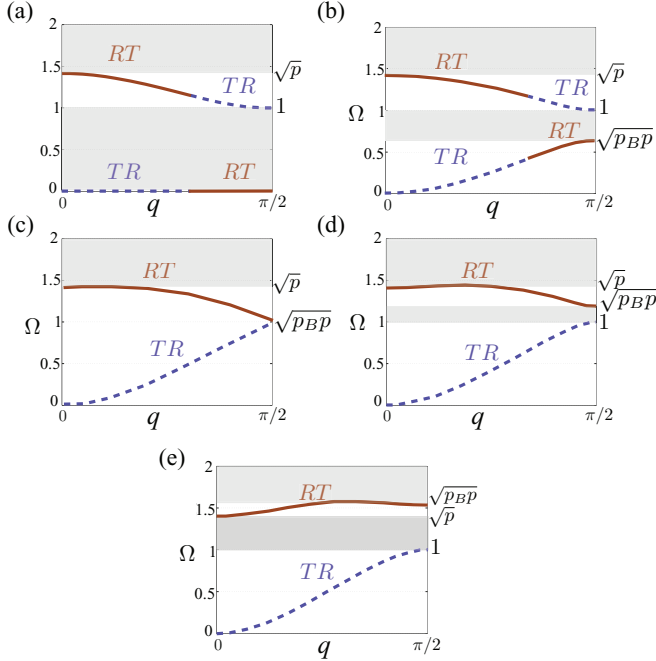
FIG. 3. (Color online) Different possible dispersion curves depending on the value of the bending rigidity parameter: $p = 2$ and (a) $p_B = 0$, (b) $0 < p_B < 1/p$ ($p_B = 0.2$), (c) $p_B = 1/p$ ($p_B = 0.5$), (d) $1/p < p_B < 1$ ($p_B = 0.7$), and (e) $p_B > 1$ ($p_B = 1.2$).
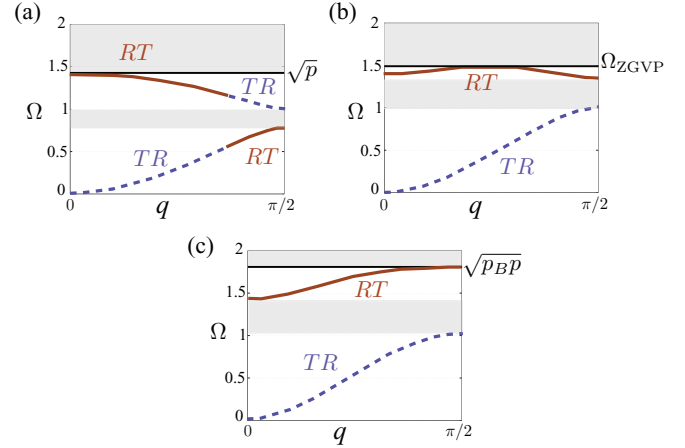

FIG. 4. (Color online) Upper limit of the second propagative band depending on the value of the bending rigidity parameter: (a) $p_B < 1 - 1/p$ ($p = 2$ and $p_B = 0.3$), (b) $1 - 1/p < p_B < 1 + 1/p$ ($p = 2$ and $p_B = 0.9$), and (c) $p_B > 1 + 1/p$ ($p = 2$ and $p_B = 1.7$).

on p and p_B. Without bending rigidity, i.e., with $p_B = 0$ [Fig. 3(a)], a counterbalance between rotational and transversal motions takes place, resulting in a zero-frequency mode called also a soft mode. As illustrated in Fig. 3(b), this mode propagates when the bending rigidity parameter p_B increases, i.e., $p_B > 0$. In fact, this counterbalance disappears due to the additional momenta ΔM acting between the particles. Two band gaps are noticed in this structure, one between the two propagating modes and one above the upper mode. The width of the band gap between the two propagating modes is described analytically. As illustrated in Fig. 3(b), when $0 < p_B < 1/p$ the lower and upper limits of the first band gap are $\sqrt{p_B p}$ and 1, respectively. When $p_B = 1/p$ the band gap closes [Fig. 3(c)]. When $1/p < p_B < 1$ the boundaries of the band gap are specified by 1 and $\sqrt{p_B p}$ [Fig. 3(d)]. Finally, when $p_B > 1$, the band gap is located between 1 and $\sqrt{p}$ [Fig. 3(e)]. Note that, by definition, p is always greater than or equal to 1.

To know the lower limit of the upper band gap, the extremum of the upper propagative band Ω_+ must be determined. The bending rigidity has an important influence on the structure of this mode. For low bending rigidities $p_B < 1 - 1/p$, the second propagating mode is monotonic with a negative group velocity and its maximum is equal to $\sqrt{p}$ [Fig. 4(a)]. For the values of p_B between $1 - 1/p$ and $1 + 1/p$ this mode becomes nonmonotonic with a zero-group-velocity point and its maximum is equal to

$$\Omega_{\mathrm{ZGVP}} = \left[\frac{4 p_B p^2}{4 p_B p - (1 + p_B p - p)^2} \right]^{1/2}$$

[Fig. 4(b)]. Finally, for the values of p_B above $1 + 1/p$ the second mode is monotonic with a positive group velocity and its maximum frequency is equal to $\sqrt{p_B p}$ [Fig. 4(c)].

III. LOCALIZED MODES

The study focuses now on the search for localized modes in the chain. With the aim of inducing localized modes, the linear chain is considered semi-infinite and a boundary condition is applied at its beginning. The analysis shows that to satisfy the boundary condition for one given frequency, two waves must be combined. As noted in Eq. (7), these two waves have wave numbers q_+ and q_-, respectively. The localized modes are, by definition, the modes whose amplitude decreases away from the boundary. Therefore, the localized wave is a combination of two evanescent waves and its decay is related to the imaginary parts of the wave numbers q_+ and q_-. Since the analysis is restricted to modes with an amplitude that decreases when n increases (to the right), the imaginary parts of the wave numbers must be negative.

In order to know at which frequency and for which parameters p and p_B the two wave numbers q_+ and q_- of the two combined waves are complex with a negative imaginary part, a description of the band structure is presented in Sec. III A. The general method to determine the frequency of the mode induced by the boundary conditions is presented in Sec. III B and the way to determine the profiles of the transversal and rotational displacements as a function of the cylinder positions is presented in Sec. III C. This method is applied to different boundary conditions in Sec. III D and the range of parameters p_B and p for which localization takes place is defined and the spatial structure of the modes is described.

A. General description of the dispersion curves

In the considered linear chain of cylinders, exhibiting two degrees of freedom each, there exist two allowed wave numbers for one single frequency (8). Depending on the value
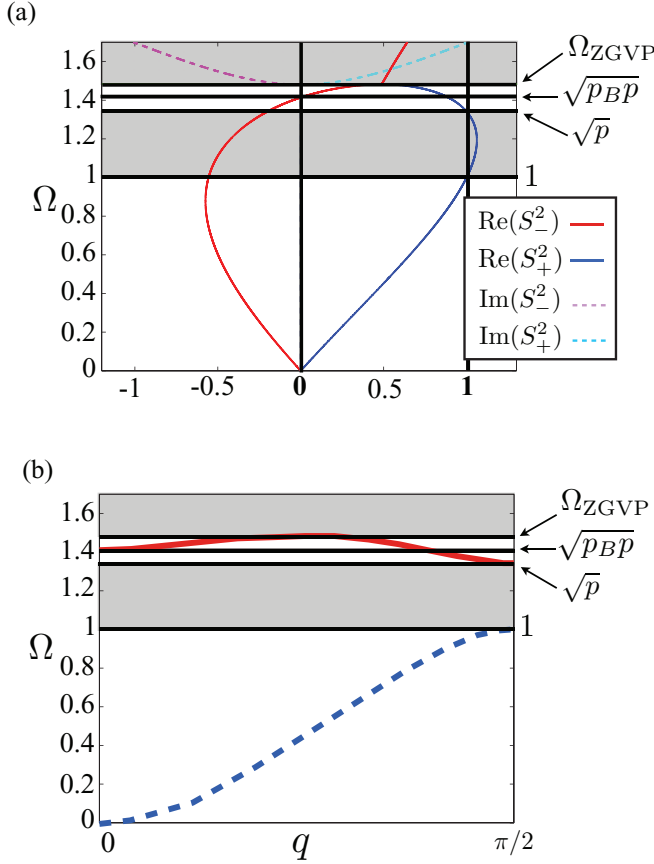
(a)

(b)

FIG. 5. (Color online) (a) Real and imaginary parts of S_+^2 and S_-^2 as a function of the frequency Ω for a homogeneous cylinder ($p = 2$) when $p_B = 0.9$. (b) Corresponding dispersion curves $\Omega = \Omega(q)$.

of the frequency, these wave numbers can be both complex, both purely real, or one complex and the other purely real. This is illustrated in Fig. 5(a), where the real and imaginary parts of S_+^2 and S_-^2 are plotted as a function of the frequency where $p = 2$ and $p_B = 0.9$. Figure 5(b) represents the corresponding dispersion curves. This description provides information about the wave numbers. On the one hand, if

$$0 \leqslant \sin^2 q \leqslant 1, \tag{11}$$

a real solution for the wave number q exists and the corresponding mode is propagative. On the other hand, if

$$\sin^2 q < 0, \ \sin^2 q > 1, \ \text{or} \ \sin^2 q = \beta' + i\beta'', \tag{12}$$

no purely real solution for q exists and the corresponding mode is evanescent.

When at least one of $S_\pm^2$ satisfies Eq. (11), the corresponding frequency Ω lies in a propagative band. When both S_+^2 and S_-^2 satisfy one of the inequalities of Eq. (12), the corresponding frequency lies in a band gap. Thus, as can be seen in Fig. 5, for example, there is one propagative and one evanescent mode in the first propagative band, i.e., when $\Omega \in [0,1]$, or two evanescent modes in the first band gap, i.e., when $\Omega \in [1, \sqrt{p}]$. See Ref. [43] for a more detailed description of S_+^2 and S_-^2 as a function of the parameters p and p_B.

Localization occurs when the frequency lies in a band gap, i.e., when the two corresponding wave numbers are complex

with a negative imaginary part. If $\sin^2 q < 0$, the wave takes the form of a simple exponential decreasing function because the wave number has an imaginary value

$$q_1 = -i \arcsinh(|H|), \tag{13}$$

where H is the square root of the right-hand side of Eq. (8). If $\sin^2 q > 1$, the wave takes the form of a decaying function with additional oscillation because the wave number has a complex value

$$q_2 = -\frac{\pi}{2} - i \arccosh(|H|). \tag{14}$$

If $\sin^2 q$ is complex, it takes the form

$$q_3 = q_3' - iq_3'', \tag{15}$$

with $q_3' = \mathrm{Re}[\arcsinh(|H|)]$ and $q_3'' = \mathrm{Im}[\arcsinh(|H|)]$, which corresponds to an exponentially decaying wave with additional oscillations. See Ref. [43] for a detailed way of determining these wave functions.

B. Determination of the frequency of the modes induced by the boundary condition

We are interested in analyzing the existence of the localized modes when the chain of cylinders is semi-infinite and one of its ends is either mechanically free or attached to an absolutely rigid wall by springs. The rigidities of these springs are, in general, different from those of the chain. Formally, both situations can be formally accessed by modifying the rigidities between the first negative and the zeroth particles in the infinite chain from $-\infty$ to ∞ for completely blocking the motion of the first negative cylinder and looking for the vibrations localized on the cylinders with non-negative n.

The shear and bending forces at the contact between the first negative and zeroth particles are described by springs of constant rigidity $\xi^{s'}$ and $\xi^{B'}$, respectively. As above, the other contacts are described with spring rigidities ξ^s and ξ^B. The new equations of motion for the particle $n = 0$ become

$$m\ddot{w}_0 = -\xi^{s'}[w_0 - w_{-1} + R_c(\varphi_0 + \varphi_{-1})]$$
$$+ \xi^s[-w_0 + w_1 + R_c(\varphi_0 + \varphi_1)], \tag{16}$$

$$I\ddot{\varphi}_0 = -\xi^{s'} R_c[w_0 - w_{-1} + R_c(\varphi_0 + \varphi_{-1})]$$
$$- \frac{(R_c\theta)^2}{2}\xi^{B'}(\varphi_0 - \varphi_{-1})$$
$$- \xi^s R_c[-w_0 + w_1 + R_c(\varphi_0 + \varphi_1)]$$
$$- \frac{(R_c\theta)^2}{2}\xi^B(\varphi_0 - \varphi_1). \tag{17}$$

Then the motion of the $n = -1$ particle is completely blocked, i.e., $w_{-1} = 0$ and $\varphi_{-1} = 0$, which mimics the absolutely rigid wall. So if $\xi^{s'} = \xi^{B'} = 0$, the beginning of the chain, starting with the zeroth particle, is mechanically free and if $\xi^{s'} \neq 0$ and $\xi^{B'} \neq 0$, the chain is attached to an absolutely rigid wall by the springs of different rigidities $\xi^{s'}$ and $\xi^{B'}$. By varying the ratio between these rigidities and those between the other cylinders of the chain, the boundary conditions are modified.

When $w_{-1} = 0$ and $\varphi_{-1} = 0$, Eqs. (16) and (17) become

$$m\ddot{w}_0 = -\xi^{s'}(w_0 + R_c\varphi_0) + \xi^s[-w_0 + w_1 + R_c(\varphi_0 + \varphi_1)], \tag{18}$$

$$I\ddot{\varphi}_0 = -\xi^{s'}R_c(w_0 + R_c\varphi_0) - \frac{(R_c\theta)^2}{2}\xi^{B'}\varphi_0$$
$$- \xi^s R_c[-w_0 + w_1 + R_c(\varphi_0 + \varphi_1)]$$
$$- \frac{(R_c\theta)^2}{2}\xi^B(\varphi_0 - \varphi_1). \tag{19}$$

Note that all the modes in the chain, i.e., both propagating and evanescent modes, satisfy the equations of motions (3) and (4). Then the difference between Eqs. (3) and (18) leads to

$$(\xi^{s'} - \xi^s)(-w_0 - \Phi_0) - \xi^s(w_{-1} - \Phi_{-1}) = 0. \tag{20}$$

Likewise, the difference between Eqs. (4) and (19) leads to

$$- \Phi_0\xi^{B'} + \Phi_0\xi^B - \Phi_{-1}\xi^B = 0. \tag{21}$$

Finally, these two boundary conditions can be rewritten as

$$(l_1 - 1)(w_0 + \Phi_0) + w_{-1} - \Phi_{-1} = 0,$$
$$(l_2 - 1)\Phi_0 + \Phi_{-1} = 0, \tag{22}$$

with $l_1 = \frac{\xi^{s'}}{\xi^s}$ and $l_2 = \frac{\xi^{B'}}{\xi^B}$.

To satisfy the system (22) two evanescent waves must be combined. The resulting mode has a displacement w_n and a rotation Φ_n of the form

$$w_n = w_{n_+} + w_{n_-} = A_+\alpha_+ e^{-i2q_+n}e^{i\omega t} + A_-\alpha_- e^{-i2q_-n}e^{i\omega t}, \tag{23}$$

$$\Phi_n = \Phi_{n_+} + \Phi_{n_-} = A_+ e^{-i2q_+n}e^{i\omega t} + A_- e^{-i2q_-n}e^{i\omega t}. \tag{24}$$

The expressions (23) and (24) are then substituted into the two conditions (22), which gives the system of equations

$$\begin{pmatrix} (l_1 - 1)(\alpha_+ + 1) + \alpha_+ e^{i2q_+} - e^{i2q_+} & (l_1 - 1)(\alpha_- + 1) + \alpha_- e^{i2q_-} - e^{i2q_-} \\ l_2 - 1 + e^{i2q_+} & l_2 - 1 + e^{i2q_-} \end{pmatrix} \begin{pmatrix} A_+ \\ A_- \end{pmatrix} = \begin{pmatrix} 0 \\ 0 \end{pmatrix}. \tag{25}$$

Solutions exist if the determinant of the matrix on the left-hand side of Eq. (25) is equal to zero. Thus the following relation between the frequency of the modes induced by the boundary condition, the ratios of the rigidities l_1 and l_2 and the wave numbers $q_\pm$, is obtained:

$$\frac{l_1\left[(C_+ - iS_+)\frac{iS_+C_+}{\Omega^2 - S_+^2}\right] - 2C_+\frac{\Omega^2}{\Omega^2 - S_+^2}}{l_1\left[(C_- - iS_-)\frac{iS_-C_-}{\Omega^2 - S_-^2}\right] - 2C_-\frac{\Omega^2}{\Omega^2 - S_-^2}} = \frac{l_2(C_+ - iS_+) + 2iS_+}{l_2(C_- - iS_-) + 2iS_-}. \tag{26}$$

When the ratios between the shear rigidities and the bending rigidities are the same, i.e., $l_1 = l_2 = l'$, the relation (26) becomes

$$\frac{iS_+C_+}{\Omega^2 - S_+^2} + \frac{l'(C_+ - iS_+) - 2C_+}{l'(C_+ - iS_+) + 2iS_+} = \frac{iS_-C_-}{\Omega^2 - S_-^2} + \frac{l'(C_- - iS_-) - 2C_-}{l'(C_- - iS_-) + 2iS_-}. \tag{27}$$

Finally, for a given l', the frequency of the possible oscillations in the chain when a boundary condition is applied at its beginning can be determined by substituting Eq. (8) into Eq. (27). Since the calculation of the general expression (for all l') of this frequency is too cumbersome, only expressions for particular values of l', i.e., for particular boundary conditions, will be given. The case of free boundary conditions ($l' = 0$) is studied in Sec. III D 1 and results by considering the link to the infinitely rigid wall to be more and more rigid ($l' > 0$) are presented in Sec. III D 2.

C. Determination of the transversal and rotational displacements of the localized modes

According to Eq. (9), the amplitudes of the transversal w_n and rotational Φ_n displacements of the localized modes as a function of the particle number n can be determined by combining two evanescent modes

$$\begin{pmatrix} w_n \\ \Phi_n \end{pmatrix} = A_+\begin{pmatrix} \alpha_+ \\ 1 \end{pmatrix}e^{-i2q_+n}e^{i\omega t} + A_-\begin{pmatrix} \alpha_- \\ 1 \end{pmatrix}e^{-i2q_-n}e^{i\omega t}. \tag{28}$$

From Eq. (25), the discrete displacements (28) can be rewritten in the form

$$\begin{pmatrix} w_n \\ \Phi_n \end{pmatrix} = A_-\left[Z\begin{pmatrix} \alpha_+ \\ 1 \end{pmatrix}e^{-i2q_+n}e^{i\Omega t} + \begin{pmatrix} \alpha_- \\ 1 \end{pmatrix}e^{-i2q_-n}e^{i\Omega t}\right], \tag{29}$$

with $Z = \frac{A_+}{A_-} = -\frac{l_2 - 1 + e^{2iq_-}}{l_2 - 1 + e^{2iq_+}}$. In the following, the normalized displacements are calculated with $A_- = 1$.

The structure of these displacements (29) as a function of the particle number depends on the wave numbers q_+ and q_- of the combined evanescent waves. The forms of these wave numbers depend on the position and value of localized mode frequency. They can take a form that corresponds to a simple exponential decaying function or to a decaying function with few oscillations. The results for different boundary conditions are presented in the next section. The existence or nonexistence of localization is described as a function of the parameters p and p_B and the profiles of the displacements are illustrated. Note that the localized modes are plotted with a dotted line to clearly show and compare the frequency value of this mode with the frequencies of the propagating modes in the following dispersion curves. However, it is important to keep in mind

that the localized mode contains two components with two different complex wave numbers.

D. Results for different boundary conditions

In this section we analyze the localization phenomena for several different particular boundary conditions applied at the beginning of the chain. In all the considered cases it is convenient to present the boundary condition (27) in the form

$$\frac{\alpha_+}{\alpha_-} = f(S_+, S_-), \tag{30}$$

where $\alpha_\pm$ are defined by Eq. (10) and f is a function dependent on the considered boundary conditions. With the notation introduced in Eq. (30), the ratio w_n/Φ_n, which provides information on the relative changes in regard to the depth n of the displacements and rotations in the localized mode, can be written as

$$\frac{w_n}{\Phi_n} = \alpha_- \frac{Z f(S_+, S_-) e^{-i2(q_+ - q_-)n} + 1}{Z e^{-i2(q_+ - q_-)n} + 1}. \tag{31}$$

Analytically, it is convenient to search for the frequencies that satisfy $(\alpha_+/\alpha_-)^2 = f^2(S_+, S_-)$ rather than Eq. (30). So when the solutions are found, we choose among them those that satisfy Eq. (30) and not $\alpha_+/\alpha_- = -f(S_+, S_-)$.

1. Free boundary condition

When $l' = 0$ and $\xi^{s'} = \xi^{B'} = 0$, the boundary of the chain is mechanically free because there is no link between the particle $n = -1$ and the particle $n = 0$. Equation (27) becomes

$$\frac{\alpha_+}{\alpha_-} = \frac{S_+^2}{S_-^2}. \tag{32}$$

By substituting the expression of $S_\pm^2$ [Eq. (8)] into Eq. (32) squared, the solutions for the mode frequencies are $\Omega_{L1_{\text{free}}}^2 = \frac{p_B p^2}{p(p_B+1)-1}$ and $\Omega_{L2_{\text{free}}}^2 = 1$. These solutions satisfy the boundary conditions (32) and thus provide the possible frequencies of the localized modes if $p_B > 1/p$.

The simple analytical expressions obtained for the propagating and localized modes provide the opportunity for a straightforward evaluation of the existence and the frequency of the localized mode depending on the relative strength of the shear and bending interparticle interactions. For a localized mode to exist, the solutions $\Omega_{L1_{\text{free}}, L2_{\text{free}}}$ should not cross the dispersion curves of the propagating modes of the infinite chain $\Omega_\pm$.

When the chain is composed of empty cylindrical shells ($p = 1$), the solutions $\Omega_{L1_{\text{free}}}$ and $\Omega_{L2_{\text{free}}}$ are equal to 1 and cannot provide localization because for all values of p_B these frequencies lie in a propagative band (Fig. 3). When $p > 1$, if a band gap exists between the two propagating modes ($p_B \neq 1/p$), the frequency $\Omega_{L1_{\text{free}}}$ always lies in the first band gap. Thus the localized vibration, composed of the two evanescent acoustic modes, exists near the mechanically free end of the chain when $p > 1$ and $p_B > 1/p$.

For the waves localized in the first band gap it is straightforward to show that w_n/Φ_n [Eq. (31)] is always
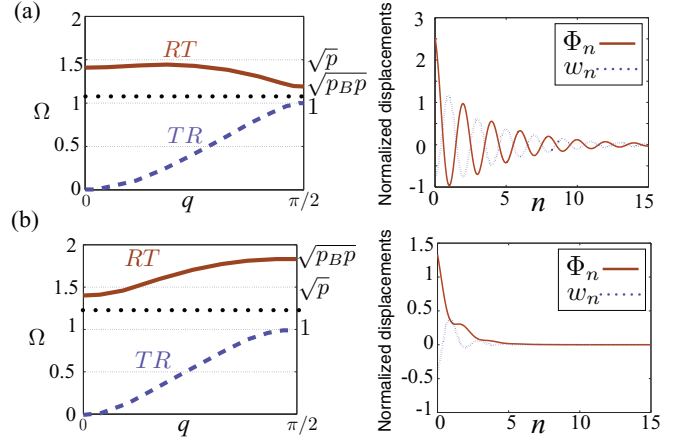

FIG. 6. (Color online) Dispersion curves and corresponding discrete displacement profiles of the localized mode in the case of free boundary conditions and for a homogenous cylinder ($p = 2$): (a) $1/p < p_B < 1$ ($p_B = 0.7$) and (b) $p_B > 1$ ($p_B = 1.7$). The solid red curves correspond to the RT mode, the dashed blue curves correspond to the TR mode, and the dotted black lines indicate the frequency value $\Omega_{L1_{\text{free}}}$.

real. For this particular boundary condition $f(S_+, S_-) \neq 1$ [Eq. (32)]. Consequently, w_n/Φ_n depends on n. In the case of the mechanically free boundary condition, in the derived localized mode, the oscillations are in antiphase ($w_n/\Phi_n < 0$) independently of n and the ratio of their amplitudes $|w_n|/|\Phi_n|$ varies with depth.

In Fig. 6 the profiles of the displacements are plotted on the right of the considered dispersion curves for homogeneous cylinders ($p = 2$) and two different values of p_B. The amplitudes of the rotational and transversal displacements of the localized mode are always a combination of a simple decaying function and a decaying function with few oscillations. As expected from a physical background, the mode is more localized, i.e., its amplitude decays more rapidly, when its frequency is far away from the two band edges. In Fig. 6(b), for $p_B > 1$, the contribution to the rotational motion of the simple exponentially decaying function is more important than the contribution of the decaying function with additional oscillations.

2. Chain in contact with rigid substrate

When $l' = 1$, the link between the chain and the rigid wall is performed via the same springs as the springs between all the other cylinders, i.e., $\xi^s = \xi^{s'}$ and $\xi^B = \xi^{B'}$. Equation (27) becomes

$$\frac{\alpha_+}{\alpha_-} = 1. \tag{33}$$

By substituting Eq. (8) into Eq. (33) squared, the solutions for the mode frequencies are $\Omega_{L1_{l'=1}}^2 = \frac{p}{1+p-p_B p}$ and $\Omega_{L2_{l'=1}}^2 = 1$. These solutions satisfy the boundary conditions (32) and thus provide the possible frequencies of the
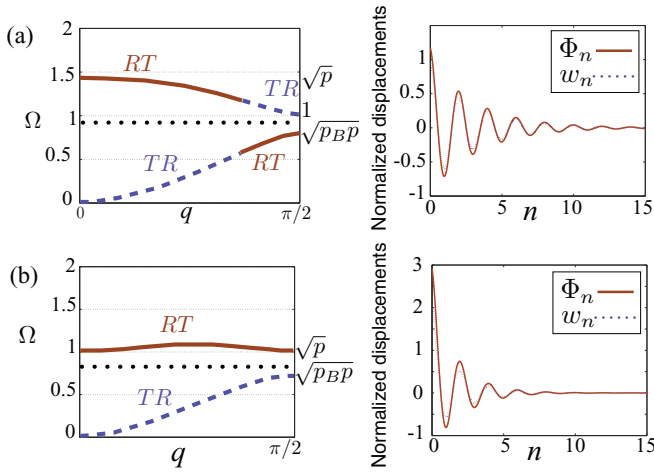
FIG. 7. (Color online) Dispersion curves and corresponding discrete displacement profiles of the localized mode when $l' = 1$ for (a) homogeneous cylinders ($p = 2$) with $p_B = 0.3 < 1/p$ and (b) empty cylindrical shells ($p = 1$) with $p_B = 0.2 < 1/p$. The solid red curves correspond to the RT mode, the dashed blue curves correspond to the TR mode, and the dotted black lines correspond to $\Omega_{L1_{l'=1}}$.

localized modes if $p_B < 1/p$. For frequency $\Omega_{L2_{l'=1}} = 1$, the mode is not localized for any values of p and p_B because this frequency always crosses a propagative band.

For $p_B < 1/p$ and for all $p \geqslant 1$, the frequency $\Omega_{L1_{l'=1}}$ is located in the first band gap. Thus, for this boundary condition, localization exists when $p_B < 1/p$ and $p \geqslant 1$ and when the frequency lies in the first band gap. Figures 7(a) and 7(b) present the dispersion curves and the corresponding profiles of the displacements in the cases of a homogeneous cylinder ($p = 2$) and an empty cylindrical cylinder ($p = 1$), respectively.

For these particular boundary conditions $f(S_+, S_-) = 1$ and Eq. (31) reduces to $w_n/\Phi_n = \alpha_-$, with $\alpha_- > 0$. Consequently, neither the relative phase nor the ratio of the amplitudes of displacements and rotations depends on n. The oscillations w_n and Φ_n are found to be in phase at all depths ($w_n/\Phi_n > 0$).

By increasing l', the link to the rigid wall becomes more rigid. For intermediate values of l' between 1 and $+\infty$, analytical expressions of the localized mode become cumbersome and the description of the existence of localization cannot be reported in detail analytically. However, it is possible to study the localization and corresponding displacements numerically. For example, with $l' = 2$, Eq. (27) becomes

$$\frac{\alpha_+}{\alpha_-} = \frac{1 - S_+^2}{1 - S_-^2}. \tag{34}$$

By substituting Eq. (8) into Eq. (34) squared, the solutions for the mode frequencies are found

$$\Omega_{L1_{l'=2}}^2 = \frac{-p(p_B + 1) + p^2(p_B^2 + p_B + 1) + \sqrt{p^2[p^2(p_B^2 + p_B + 1)^2 - 2p(p_B^3 + 1) + (p_B - 1)^2]}}{2(p_B p + p - 1)},$$

$$\Omega_{L2_{l'=2}}^2 = \frac{-p(p_B + 1) + p^2(p_B^2 + p_B + 1) - \sqrt{p^2[p^2(p_B^2 + p_B + 1)^2 - 2p(p_B^3 + 1) + (p_B - 1)^2]}}{2(p_B p + p - 1)}.$$

These solutions satisfy the boundary conditions (32) and thus provide the possible frequencies of the localized modes for all values of p and p_B.

The frequency $\Omega_{L2_{l'=2}}$ is not real and the frequency $\Omega_{L1_{l'=2}}$ can be found in the upper band gap when $p_B > 0$ and for different values of p. The description of S_+^2 and S_-^2 in the upper band gap [43] provides an opportunity to describe the profiles of the displacements depending on the value of the parameters.

Three different cases are possible: either $S_+^2 < 0$ and $S_-^2 < 0$, or S_+^2 and S_-^2 are complex, or $S_+^2 > 1$ and $S_-^2 > 1$. See Ref. [43] for a description of the values of the parameters p and p_B corresponding to these three cases.

Examples of dispersion curves and corresponding profiles of displacements are depicted in Fig. 8 for these three cases. Figure 8(a) corresponds to the case where $S_+^2 < 0$ and $S_-^2 < 0$. In this case, the wave numbers q_+ and q_- constituting the localized mode are both in the form of Eq. (13), which corresponds to a simple exponentially decreasing wave function. The oscillations are in phase ($w_n/\Phi_n > 0$ and real) independently of n and the ratio of their amplitudes $|w_n|/|\Phi_n|$ varies with depth.

Figure 8(b) corresponds to the case where S_+^2 and S_-^2 are complex. The wave numbers are both in the form of Eq. (15), which corresponds to a decaying wave function with additional

oscillations. The values of w_n/Φ_n are complex and depend on n, i.e., the relative phase and the ratio of the amplitudes depend on n.

Figure 8(c) corresponds to the case where $S_+^2 > 1$ and $S_-^2 > 1$. The wave numbers constituting the localized mode are both in the form of Eq. (14), which corresponds to a decaying wave function with additional oscillations. The oscillations are in antiphase ($w_n/\Phi_n < 0$ and real) independently of n and the ratio of their amplitudes $|w_n|/|\Phi_n|$ varies with depth. When the bending rigidity increases [Fig. 8(c)], the transversal displacement vanishes and the rotational motion is dominant.

When $l' \to +\infty$, Eq. (27) becomes

$$\frac{\alpha_+}{\alpha_-} = \frac{S_+^2}{S_-^2}.$$

This case is identical to the one with $l' = 1$, except that the localization will start from the $n = 1$ particle. In fact, by increasing l' the link to the wall at the $n = -1$ particle becomes more and more rigid and finally, when $l' \to +\infty$, the motion of the zeroth particle is completely blocked and the zeroth cylinder becomes part of the rigid wall.
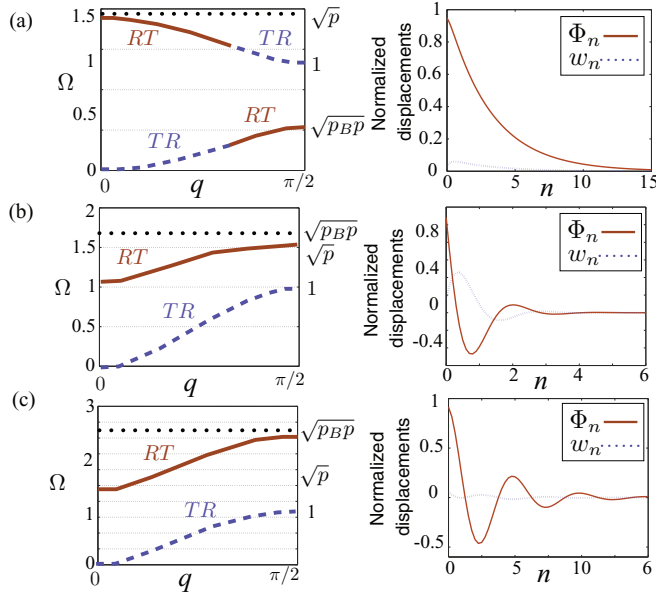
FIG. 8. (Color online) Dispersion curves and discrete rotational and transversal displacements when $l' = 2$ and (a) $p = 2$ and $p_B = 0.08$, (b) $p = 1.2$ and $p_B = 2$, and (c) $p = 2$ and $p_B = 2.95$.

IV. CONCLUSION

In this work we have demonstrated that localized modes can be exhibited in a 2D monatomic granular crystal when transversal and rotational motions are considered. The chain is composed of cylinders of equal mass, which possess one translational and one rotational degree of freedom. The interaction between transversal and rotational waves leads to two dispersive propagating acoustic modes, separated by a gap of forbidden frequencies. By modifying the bending and shear rigidities between the end of the chain and a rigid wall, we have established the required conditions for the existence of a localized mode in the semi-infinite chain of cylinders. The special feature of the evaluated linear chain of cylinders, exhibiting two degrees of freedom each, is that the localized mode is composed of two evanescent modes.

This is an important difference from earlier studied cases of longitudinal localized modes in linear chains of beads and in layered structures where at each frequency only a single evanescent mode could exist. The advantage of this theoretical evaluation of discrete granular crystal is to obtain simple analytical expressions for the propagating and localized modes. Depending on the ratio between the rigidities of the springs connecting the first cylinder in the chain to the rigid wall and the rigidities between the other cylinders of the chain, the frequency of the localized mode can lie either in the forbidden band between the two propagating modes or above the upper propagating mode. We have examined the profiles of the rotational and transversal displacements of the localized mode as a function of the particle number and for different boundary conditions. Depending on the position of the localized mode frequency with respect to the propagating bands, these profiles and the degree of localization are various. The results of our research, the mode localization in a chain with cylinders of equal mass, are complementary to the recent theoretical [28,31,32] and experimental [33] investigations of the acoustic waves in 2D and 3D granular crystals where the roles of the rotational degrees of freedom of the beads on the wave propagation have been analyzed.

In the future, this investigation should be extended to two- and three-dimensional granular crystals in terms of the wedge and the surface waves characterizing these structures and also to comparison of these surface waves with the prediction of surface modes existing within the Cosserat continuum. In the experimental investigations of these localized modes the considered configuration would be realized using a chain composed of magnetic cylinders. To investigate the vibrational response of the chain, it can be excited at one of its ends by a shaker. The attractive magnetic force between cylinders causes in this case the prestress of the contacts between the cylinders, initiating their shear and bending contact rigidities.

[1] M. Cai, O. Painter, and K. J. Vahala, Phys. Rev. Lett. **85**, 74 (2000).

[2] F. de Fornel, *Evanescent Waves: From Newtonian Optics to Atomic Optics* (Springer, New York, 2001).

[3] C. Spielmann, R. Szipöcs, A. Stingl, and F. Krausz, Phys. Rev. Lett. **73**, 2308 (1994).

[4] S. Yang, J. H. Page, Z. Liu, M. L. Cowan, C. T. Chan, and P. Sheng, Phys. Rev. Lett. **88**, 104301 (2002).

[5] J. B. Pendry, Phys. Rev. Lett. **85**, 3966 (2000).

[6] D. M. Profunser, O. B. Wright, and O. Matsuda, Phys. Rev. Lett. **97**, 055502 (2006).

[7] R. J. P. Engelen, D. Mori, T. Baba, and L. Kuipers, Phys. Rev. Lett. **102**, 023902 (2009).

[8] J. Mahanty, A. A. Maradudin, and G. H. Weiss, Prog. Theor. Phys. **20**, 1 (1958).

[9] V. Keppens, D. Mandrus, B. Sales, B. Chakoumakos, P. Dai, R. Coldea, M. Maple, D. Gajewski, E. Freeman, and S. Bennington, Nature (London) **395**, 876 (1998).

[10] J. J. Mock, R. T. Hill, Y.-J. Tsai, A. Chilkoti, and D. R. Smith, Nano Lett. **12**, 1757 (2012).

[11] E. W. Montroll and R. B. Potts, Phys. Rev. **100**, 525 (1955).

[12] R. F. Wallis and A. A. Maradudin, Prog. Theor. Phys. **24**, 1055 (1960).

[13] R. L. Bjork, Phys. Rev. **105**, 456 (1957).

[14] R. F. Wallis, Phys. Rev. **105**, 540 (1957).

[15] R. E. Camley, B. Djafari-Rouhani, L. Dobrzynski, and A. A. Maradudin, Phys. Rev. B **27**, 7318 (1983).

[16] E. H. El Boudouti, B. Djafari-Rouhani, A. Akjouj, and L. Dobrzynski, Phys. Rev. B **54**, 14728 (1996).

[17] H. J. Trodahl, P. V. Santos, G. V. M. Williams, and A. Bittar, Phys. Rev. B **40**, 8577 (1989).

[18] S. Mizuno and S. I. Tamura, Phys. Rev. B **53**, 4549 (1996).

[19] H. T. Grahn, J. Maris, J. Tauc, and B. Abeles, Phys. Rev. B **38**, 6066 (1988).

[20] N.-W. Pu and J. Bokor, Phys. Rev. Lett. **91**, 076101 (2003).

[21] S. Aubin, P. B. Allen, and R. B. Doak, Am. J. Phys. **68**, 228 (2000).

[22] A.-C. Hladky-Hennion, A. Devos, and M. de Billy, J. Acoust. Soc. Am. **116**, 117 (2004).

[23] A.-C. Hladky-Hennion, G. Allan, and M. de Billy, J. Appl. Phys. **98**, 054909 (2005).

[24] A.-C. Hladky-Hennion and M. de Billy, J. Acoust. Soc. Am. **122**, 2594 (2007).

[25] G. Theocharis, N. Boechler, P. G. Kevrekidis, S. Job, M. A. Porter, and C. Daraio, Phys. Rev. E **82**, 056604 (2010).

[26] N. Boechler, G. Theocharis, S. Job, P. G. Kevrekidis, M. A. Porter, and C. Daraio, Phys. Rev. Lett. **104**, 244302 (2010).

[27] C. Hoogeboom, G. Theocharis, and P. G. Kevrekidis, Phys. Rev. E **82**, 061303 (2010).

[28] A. Merkel, V. Tournat, and V. Gusev, Phys. Rev. E **82**, 031305 (2010).

[29] V. Nesterenko, *Dynamics of Heterogeneous Materials* (Springer, New York, 2001).

[30] K. Johnson, *Contact Mechanics* (Cambridge University Press, Cambridge, 1987).

[31] V. Tournat, I. Pèrez-Arjona, A. Merkel, V. Sanchez-Morcillo, and V. Gusev, New J. Phys. **13**, 073042 (2011).

[32] H. Pichard, A. Duclos, J.-P. Groby, V. Tournat, and V. E. Gusev, Phys. Rev. B **86**, 134307 (2012).

[33] A. Merkel, V. Tournat, and V. Gusev, Phys. Rev. Lett. **107**, 225502 (2011).

[34] A. Eringen, *Microcontinuum Field Theories. I. Foundations and Solids* (Springer, New York, 1999).

[35] W. Nowacki, *Theory of Asymmetric Elasticity* (Pergamon, Oxford, 1986).

[36] M. Kulesh, V. P. Matveenko, and I. Shardakov, Acoust. Phys. **52**, 186 (2006).

[37] Y. D. Chong, X.-G. Wen, and M. Soljacic, Phys. Rev. B **77**, 235125 (2008).

[38] T. Ochiai, J. Phys.: Condens. Matter **22**, 225502 (2010).

[39] C. Ouyang, D. Han, F. Zhao, X. Hu, X. Liu, and J. Zi, J. Phys.: Condens. Matter **24**, 492203 (2012).

[40] Y.-t Fang, X.-h Song, L.-z Lu, J.-j Wang, Y.-x Jiang, and M. Zhu, Opt. Commun. **228**, 129 (2013).

[41] D. Jukić, H. Buljan, D.-H. Lee, J. D. Joannopoulos, and M. Soljacic, Opt. Lett. **37**, 5262 (2012).

[42] A. Suiker, A. Metrikine, and R. de Borst, Int. J. Solids Struct. **38**, 1563 (2001).

[43] See Supplemental Material at http://link.aps.org/supplemental/ 10.1103/PhysRevE.89.013201 for a detailed description of the dispersion curves and details of some calculations.